Human-relevant near-organ neuromodulation of the immune system via the splenic nerve

Matteo Donegà[a,1,2], Cathrine T. Fjordbakk[b,1], Joseph Kirk[b], David M. Sokal[a], Isha Gupta[a], Gerald E. Hunsberger[a], Abbe Crawford[b], Simon Cook[b], Jaime Viscasillas[b], Thaleia-Rengina Stathopoulou[b], Jason A. Miranda[a], Wesley J. Dopson[a], David Goodwin[b], Alison Rowles[c], Paul McGill[d], Alex McSloy[b], Dirk Werling[e], Jason Witherington[a], Daniel J. Chew[a], and Justin D. Perkins[b,2]

[a]Translation and Engineering, Galvani Bioelectronics, Stevenage SG1 2NY, United Kingdom; [b]Clinical Sciences and Services, The Royal Veterinary College, Hatfield AL9 7TA, United Kingdom; [c]Non-Clinical Safety, GlaxoSmithKline, Ware SG12 0DP, United Kingdom; [d]Bioimaging, GlaxoSmithKline, Ware SG12 0DP, United Kingdom; and [e]Department of Pathobiology and Population Sciences, Royal Veterinary College, Hatfield AL9 7TA, United Kingdom

Edited by Clifford J. Woolf, Boston Children's Hospital and Harvard Medical School, Boston, MA, and accepted by Editorial Board Member Ruslan Medzhitov March 30, 2021 (received for review December 17, 2020)

Neuromodulation of immune function by stimulating the autonomic connections to the spleen has been demonstrated in rodent models. Consequently, neuroimmune modulation has been proposed as a new therapeutic strategy for the treatment of inflammatory conditions. However, demonstration of the translation of these immunomodulatory mechanisms in anatomically and physiologically relevant models is still lacking. Additionally, translational models are required to identify stimulation parameters that can be transferred to clinical applications of bioelectronic medicines. Here, we performed neuroanatomical and functional comparison of the mouse, rat, pig, and human splenic nerve using in vivo and ex vivo preparations. The pig was identified as a more suitable model of the human splenic innervation. Using functional electrophysiology, we developed a clinically relevant marker of splenic nerve engagement through stimulation-dependent reversible reduction in local blood flow. Translation of immunomodulatory mechanisms were then assessed using pig splenocytes and two models of acute inflammation in anesthetized pigs. The pig splenic nerve was shown to locally release noradrenaline upon stimulation, which was able to modulate cytokine production by pig splenocytes. Splenic nerve stimulation was found to promote cardiovascular protection as well as cytokine modulation in a high- and a low-dose lipopolysaccharide model, respectively. Importantly, splenic nerve–induced cytokine modulation was reproduced by stimulating the efferent trunk of the cervical vagus nerve. This work demonstrates that immune responses can be modulated by stimulation of spleen-targeted autonomic nerves in translational species and identifies splenic nerve stimulation parameters and biomarkers that are directly applicable to humans due to anatomical and electrophysiological similarities.

splenic nerve | vagus nerve | neuromodulation | immunomodulation

The inflammatory status of the body is monitored and regulated through the neuroimmune axis, connecting the brain to the immune system via both humoral and neural pathways (1–3). In particular, the inflammatory reflex (3) controls systemic immune responses; detection of inflammatory stimuli in the periphery is communicated to the brain that activates outflow of neural signals to promote peripheral immune responses proportional to the threat. Studies in rodent models have identified the cholinergic anti-inflammatory pathway (CAIP) as the brain's efferent response to infection and inflammation through peripheral neurotransmitters released in lymphoid organs, mainly the spleen (4, 5). Within this pathway, the peripheral connection between the vagus nerve (VN), the splenic nerve (SpN), and its terminal release of noradrenaline (NA) into the spleen have been identified as crucial components of this neural circuit (6–8) (*SI Appendix*, Fig. S1*A*).

Importantly, the CAIP can be harnessed to promote immune control. Activation of the cervical VN by electrical stimulation (vagus nerve stimulation—VNS; *SI Appendix*, Fig. S1*A*) has been shown to be effective in reducing lipopolysaccharide (LPS)-induced levels of tumor necrosis factor alpha (TNF-α) (4, 6, 7) and in preclinical rodent models of chronic inflammatory diseases (9, 10). Murine models have generally been used to demonstrate biological proof of concepts of novel neuromodulation therapies in this and other contexts. However, the development of clinical bioelectronic medicines requires the accurate estimation and validation of stimulation parameters in a histologically, surgically, and anatomically relevant model to define device and therapy requirements. The translation of stimulation parameters from rodent to human is hampered by anatomical (e.g., size of nerves), histological (e.g., number of axons, connective tissue thickness, proportion of adipose tissue), and physiological (e.g., immunological) differences. Therefore, it is suggested that the use of large animal models, human tissues, and in silico modeling

Significance

Bioelectronic modulation of the autonomic nervous system innervating the spleen represents a new therapeutic avenue. Studies in rodents suffer from the limitation that stimulation parameters and anatomy are not directly applicable to humans. This work demonstrates the translation of biological mechanisms in a large animal model with similar anatomical, histological, and functional characteristics for derivation of human-relevant parameters. Here, we show the scientific process for translating a bioelectronic medicine to clinical readiness. The results presented can be used in three ways: 1) as a system to demonstrate the species translation of neuroimmune modulation, 2) as an exemplar of how translational models can reveal additional potential mechanisms, and 3) as a general methodology to determine human-relevant stimulation parameters.

Author contributions: M.D., C.T.F., D.W., J.W., D.J.C., and J.D.P. designed research; M.D., C.T.F., J.K., D.M.S., I.G., G.E.H., A.C., S.C., J.V., T.-R.S., J.A.M., W.J.D., D.G., A.R., P.M., A.M., and J.D.P. performed research; M.D., C.T.F., J.K., I.G., G.E.H., S.C., A.M., and D.W. analyzed data; and M.D., C.T.F., and D.M.S. wrote the paper.

Competing interest statement: M.D., I.G., D.M.S., J.A.M., W.J.D., J.W., D.J.C., and G.E.H. are employees of Galvani Bioelectronics and declare that some of the work described in this publication is the subject matter of pending patent applications. C.T.F., D.G., J.K., A.M., and J.D.P. declare that Galvani Bioelectronics provided funds to support their work associated with this manuscript.

This article is a PNAS Direct Submission. C.J.W. is a guest editor invited by the Editorial Board.

[1]M.D. and C.T.F. contributed equally to this work.

[2]To whom correspondence may be addressed. Email: matteo.donega@gmail.com or JPerkins@rvc.ac.uk.

This article contains supporting information online at https://www.pnas.org/lookup/suppl/doi:10.1073/pnas.2025428118/-/DCSupplemental.

Published May 10, 2021.

are more appropriate for the optimization and scaling of human-relevant parameters (11, 12).

Although early clinical feasibility studies have provided preliminary evidence of immunomodulatory effects of VNS in patients (13, 14), clear demonstration of the translation of the splenic anti-inflammatory pathway in clinically relevant species is currently lacking in the literature. The VN has a functionally and anatomically complex composition. In animals and humans, the VN contains both afferent and efferent axons of varying size (large, medium, and small) and degree of myelination (heavily myelinated, lightly myelinated, and unmyelinated axons) innervating multiple organs and muscles (15). As a consequence, currently used VNS results in activation of off-target circuits (*SI Appendix*, Fig. S1*A*) that can cause dysphonia, coughing, hoarseness, pain, and dyspnea (16–18); in some patients, these can be managed and can also improve over time (18). Further, it remains unclear which axons (efferent versus afferent, myelinated versus unmyelinated) within the VN relay immunomodulatory signals to peripheral organs (19, 20). As a result, it is difficult to optimize the stimulation parameters necessary to activate axons within the VN which carry signals to the spleen. Typically, clinical parameters are selected based on the individual patient's tolerance of off-target effects (13, 21) without direct evidence of activation of the anti-inflammatory pathway because of a lack of an organ-specific biomarker. Since the SpN directly transmits neural signals to the spleen and is the fundamental nodal circuit in mediating the anti-inflammatory response (22), SpN stimulation (SpNS) may represent an alternative modality providing the opportunity for near-organ modulation of the immune system (*SI Appendix*, Fig. S1 *B* and *C*). Proof of concept experiments in rodents have shown that immune responses can indeed be modulated by stimulation of the SpN with comparable cytokine suppressive effects to VNS (7, 8, 23).

Here, we anatomically, histologically, and functionally compared the mouse, rat, pig, and human SpN, demonstrating the superiority of the pig as a translational model of the human SpN. We then performed functional in vivo pig electrophysiological studies to identify organ-specific physiological biomarkers that can be used to assess nerve engagement and to refine stimulation parameters. Finally, we assessed the large animal translation of the spleen-dependent anti-inflammatory pathway in the pig using in vitro splenocyte preparations together with two in vivo models of acute inflammation.

Results

Gross Anatomy and Histology of the Splenic Neurovascular Bundle. Cadaveric studies in rats showed that the splenic artery (SpA) originates from the celiac artery and courses as a single vessel (common SpA) for a short distance (length: 1 to 3 mm) prior to separating into two major branches: a dorsal and a ventral branch (Fig. 1*A*), which also supply the stomach and pancreas, respectively, before entering the splenic parenchyma (Fig. 1*A*). The mouse SpA anatomy presented with the same branching pattern; however, the common SpA is generally absent or very short (<1 mm). In both rodent species, the splenic vein (SpV) has a similar architecture, with the dorsal and ventral branches running in close proximity to the SpA toward the hepatic portal vein (Fig. 1*A*). Nerve fascicles comprising the mouse and rat SpN plexus, arising from the celiac-mesenteric ganglion (CG), coursed along the SpA toward the spleen. Additionally, the base of the spleen receives innervation from a separate nerve different from the main plexus running along the SpA (*SI Appendix*, Fig. S2*A*) as recently described (24).

In contrast, the SpA of farm pigs (45 to 55 kg body weight) originates from the celiac artery but courses as a single artery (length: 40 to 55 mm), reaching the splenic hilum (Fig. 1*B* and *SI Appendix*, Fig. S2*C*) in accordance with previous literature (25). At the hilum, one smaller dorsal arterial branch exits the SpA and travels toward the splenic base, where it divides into several smaller short gastric arteries coursing toward the stomach (Fig. 1*B*). The main SpA continues ventrally along the visceral surface of the spleen, supplying the organ throughout its length. The left gastroepiploic artery branches off this ventral portion of the SpA (Fig. 1*B*). The SpV presents a similar architecture, with short gastric and gastroepiploic veins feeding into the SpV running along the SpA until diverging in a cranial direction toward the hepatic portal vein. The SpN was observed as a plexus comprising multiple discrete and interconnecting nerve fascicles coursing along the SpA and originating from the CG (Fig. 1*B* and *SI Appendix*, Fig. S2*C*). Nerves were only observed along the arterial supply, and no additional nerve connections were observed.

Similar to the pig, the human SpA also originates from the celiac artery and runs typically as a single vessel toward the spleen until branching into superior and inferior branches that enter the splenic hilum (Fig. 1*C*) and short gastric and gastroepiploic arteries supplying the stomach. The human organ donor tissues investigated (*SI Appendix*, Table S1) in the current study displayed SpAs of variable tortuosity (*SI Appendix*, Fig. S2*F*) and length in line with published literature (26, 27). The human SpN, known to originate from the CG (28), was observed as a plexus coursing along and around the SpA as in the other species.

The intricate structure formed by the SpN plexus and the SpA is hereafter referred to as the splenic neurovascular bundle (NVB).

Histomorphometric Analysis of Splenic NVB. In all the investigated species, the SpN was observed as a circumferential periarterial plexus (Fig. 1 *D–F*). Detailed histomorphometric analysis of the mouse, rat, pig, and human splenic NVB was performed at the regions illustrated in Fig. 1 *A–C* (*Materials and Methods*). In all species, NVB dimensions (external SpA diameter, number, and size of SpN fascicles) were larger proximally (closer to the celiac origin) than distally (closer to the spleen) (Fig. 1 *G–I*). This is exemplified by the measurements in the rat in which the common SpA diameter was between 1.3 to 2.6 times larger than the ventral and dorsal SpA (mean ± SD: 361.1 ± 121.8 μm versus 245.7 ± 49.5 and 125.9 ± 19.7 μm, respectively), whereas the number of fascicles, the fascicle diameter, and the distance from the arterial wall were between 1.5 to 6 times larger proximally than distally (Fig. 1 *G–I*). Furthermore, the mouse ventral and dorsal SpA diameters were half the size of the corresponding structures in the rat, whereas all other parameters quantified were more than two times smaller in the mouse versus the rat.

In order to perform a relevant comparison between species, the common SpA region of the rat NVB was compared to the middle SpA portion of the pig and human tissues, the site of stimulation in the subsequent functional experiments. At these locations, the human SpA diameter (4.7 ± 0.4 mm) was twice the size of the pig (2.1 ± 0.3 mm) but one order of magnitude larger than the rat (361.1 ± 121.8 μm) common SpA. Additional samples collected from larger pigs (70 to 110 kg body weight) showed a range of SpA diameters (4 to 6.5 mm) in line with the human samples. The number of SpN fascicles of the human NVB was similar to the pig but twice that of the rat NVB (Fig. 1*G*). The mean fascicle diameter was instead 1.3 times higher in the pig as compared to the human and two times higher than the rat SpN (Fig. 1*H*). Finally, in all animal models, the SpN plexus was embedded in connective tissue, whereas the human samples also presented with variable amounts of adipose tissue (Fig. 1*F* and *SI Appendix*, Fig. S2*F*). As a consequence, the mean distance from the fascicles to the arterial wall was three to four times higher in human than in pig and rat. Across all parameters, the distal portion of the NVB in human and pig samples was characterized by significantly higher values as compared to both rats and mice.

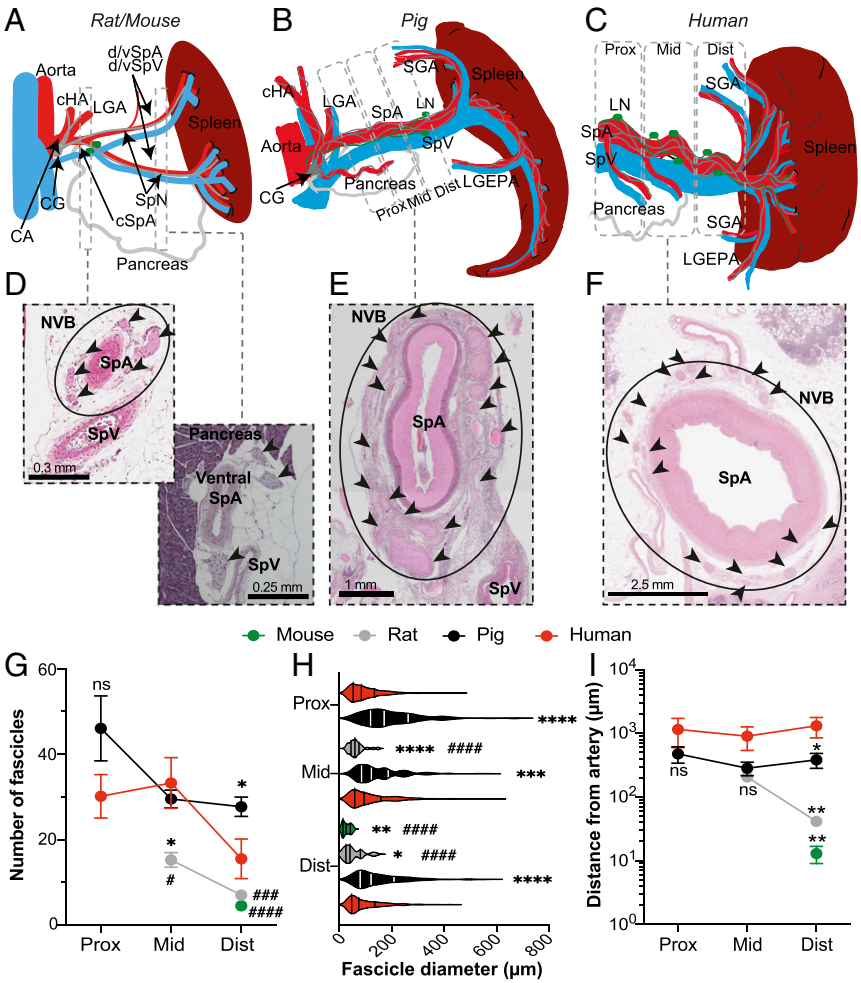

Fig. 1. Characterization of splenic NVB across species. (*A–C*) Schematic of the mouse, rat, pig, and human neurovascular anatomy. The dashed lines delineate the level of the splenic NVB where the histological sections were collected and quantified. (*D–F*) Representative sections of splenic NVB from (*D*) rat (common and ventral SpA), (*E*) pig (middle SpA), and (*F*) human (middle SpA). The sections were stained with Hematoxylin and Eosin. The arrow heads indicate the individual fascicles, and the ovals indicate the region referred to as splenic NVB. (*G–I*) Quantification of (*G*) the number of fascicles, (*H*) fascicle diameter, and (*I*) distance from the artery wall of the SpN in the four species from n = 4 (rat and mouse) or n = 6 (pig and human) tissue donors at the different locations: proximal (prox), middle (mid), and distal (dist). For rats and mice, the middle location indicates the common SpA, and the distal indicates the dorsal/ventral region of SpA. Data in *G* and *I* are shown as mean ± SEM. Data in *H* are shown as a violin plot distribution with median and interquartile range. $*P \leq 0.05$ or $\#P \leq 0.05$; $**P \leq 0.01$ or $\#\#P \leq 0.01$; $***P \leq 0.001$ or $\#\#\#P \leq 0.001$; $****P \leq 0.0001$ or $\#\#\#\#P \leq 0.0001$. *, difference versus human; #, difference versus pig. CA = celiac artery; CG = celiac ganglion; cHA = common hepatic artery; LGA = left gastric artery; LGEPA = left gastroepiploic artery; LN = lymph node; NVB = neurovascular bundle; SGA = short gastric arteries; SpA = splenic artery; SpN = splenic nerve; SpV = splenic vein.

Comparison of SpN Charge Requirements across Species. Due to the periarterial circumferential distribution of SpN fascicles, a peri-arterial cuff electrode incorporating the NVB was selected as a suitable neural interface for stimulation across species (*SI Appendix*, Fig. S2 *B–J*). Due to the lack of an interface point comparable to the other species and the spatial restriction of its splenic neuroanatomy not permissive to implantation of both stimulating and recording electrodes, the mouse was excluded from these experiments. Consequently, in vivo electrophysiological experiments were performed in terminally anesthetized rats and pigs as depicted in *SI Appendix*, Fig. S2 *H* and *I*. Bipolar electrical SpNS was applied at 1 Hz, with various pulse widths (PW) and stimulation amplitudes, and the evoked compound action potential (eCAP) was recorded (Fig. 2 *A* and *B*, *Left*). In the pig, stimulation was also applied to discrete isolated SpN fascicles dissected free from the SpA immediately proximal to the recording electrodes as a control (Fig. 2*B*). Recordings of eCAP demonstrated a typical strength–duration relationship between current amplitude for nerve recruitment and PW when stimulating the splenic NVB in both animal models (Fig. 2 *A* and *B*, *Right*). The mean calculated SpN conduction velocity was found to be 0.72 m/sec in both animal models (range: 0.57 to 0.9 m/sec in the pig and 0.58 to 0.88 m/sec in the rat) (Fig. 2*D*).

In order to investigate the clinical relevance of the charge required to stimulate the pig and rat SpN, we compared ex vivo electrophysiological data recently obtained from donor-derived human NVB (*SI Appendix*, Fig. S2 *F* and *G*) (12) against the pig and rat in vivo data. In line with the pig experiments, both the NVB and isolated nerve fascicles were stimulated in human tissues, and the eCAP was recorded (*SI Appendix*, Fig. S2*J* and Fig. 2*C*). The mean conduction velocity of the human SpN was found to be 0.46 m/sec (range 0.41 to 0.49 m/sec), which was significantly slower than that in the pig and rat (Fig. 2*D*). This may in part be due to temperature differences between the in vivo (36 to 37 °C) and the ex vivo (25 to 30 °C) experiments. When comparing the charge requirement for activation of the

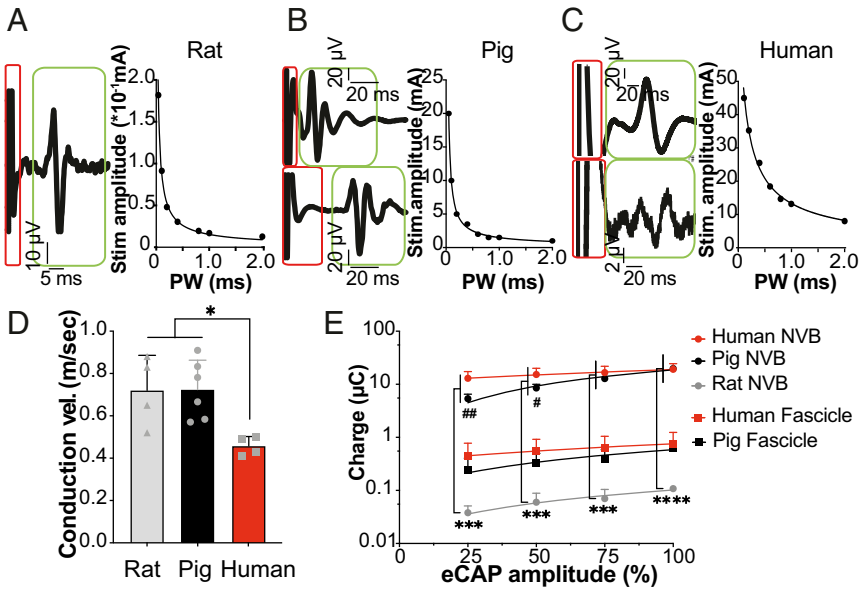

Fig. 2. The pig SpN mimics the human stimulation charge requirements. (*A–C*, *Left*) Representative traces of the SpN eCAP recorded when stimulating the NVB or when stimulating the discrete fascicles (*Bottom* for pig and human) in (*A*) rats, (*B*) pigs, (*C*) and human tissues. Traces are the average of eight consecutive monophasic stimulation pulses delivered at 1 Hz. (*A–C*, *Right*) The graphs show the strength–duration relationship (current amplitude versus PW) of the rat, pig, and human SpN obtained by stimulating the NVB in all species. An exponential decay curve was plotted against the strength–duration data. Data are shown as mean (n ≥ 3). (*D*) Conduction velocity of the SpN in the three different species. Individual values, with mean + SD are shown. (*E*) Graph comparing the charge requirements to activate 25, 50, 75, and 100% of the axons when stimulating the NVB (circles) in human (red), pig (black), and rat (gray) SpN. The charge to stimulate discrete fascicles for the human and the pig SpN is also shown (squares). Data are shown as mean (n ≥ 3) + SD $*P \leq 0.05$ or $\#P \leq 0.05$; $**P \leq 0.01$ or $\#\#P \leq 0.01$; $***P \leq 0.001$; $****P \leq 0.0001$. #, difference between human and pig NVB. More extensive data and analysis on human samples were recently published elsewhere (12).

NVB among the three species, the rat was found to be two orders of magnitude smaller than the charge required for the human and the pig (Fig. 2*E*). The charge required to activate the rat NVB was also one order of magnitude smaller than that required for a single isolated human or porcine fascicle (Fig. 2*E*). There was little difference between human and pig charge requirements for NVB or fascicle activation. At nerve activation levels <50%, a statistically higher charge requirement was observed for the human tissues; however, this difference was small in magnitude. At activation levels >50%, charge requirements were found to be equal between the two species (Fig. 2*E*).

Taken together, these anatomical, histological, and electrophysiological data demonstrate that the pig is a more similar model of the human splenic NVB than the rat or mouse.

Physiological Biomarkers of Splenic Nerve Stimulation in the Pig. Preliminary experiments in anesthetized rats showed that electrical stimulation of the SpN (bipolar, biphasic, symmetrical rectangular pulses, 0.4 ms PW, 10 Hz) caused a stimulation (measured as charge) amplitude-dependent reduction of SpA mean blood flow (mBF), initiating soon after stimulation onset and returning to baseline levels (defined as average of the 30 s prior to stimulation onset) following cessation of stimulation (*SI Appendix*, Fig. S3*A*). As a consequence, we then sought to determine the stimulation-induced changes in pig physiology to validate and characterize target-specific biomarkers of nerve engagement. In line with the rat, stimulation of the pig splenic NVB (using bipolar electrodes and symmetric, biphasic rectangular pulses delivered at 0.4 ms PW and varying frequencies and amplitudes) evoked a transient reduction of SpA mBF (Fig. 3*A*). The SpA mBF reached a minimum within 15 to 30 s of stimulation onset, after which it stabilized for the remaining stimulation period and returned to baseline levels typically within 60 to 180 s after cessation of stimulation (Fig. 3*A*). The reduction was shown to be stimulation amplitude (*SI Appendix*, Fig. S3*B*) and frequency (*SI Appendix*, Fig. S3 *C* and *D*) dependent. At a constant stimulation frequency of 10 Hz, the maximum reduction in SpA mBF was obtained at a stimulation amplitude corresponding to the maximum level of simultaneously recorded eCAP (Fig. 3*B*).

The stimulation also caused visible splenic capsular contraction in pigs, quantified by changes in SpV mBF. This showed an immediate increase followed by a reduction to below baseline levels in line with the reduced inflow (reduction in SpA mBF) (Fig. 3*A*). The increase in SpV mBF was also amplitude and frequency dependent (Fig. 3*B* and *SI Appendix*, Fig. S3*F*). In parallel, we also monitored and quantified changes in systemic parameters. Stimulation of the SpN in pigs caused transient systemic cardiovascular responses (Fig. 3*A*), including an amplitude- (*SI Appendix*, Fig. S3*E* and Fig. 3*B*) and frequency- (*SI Appendix*, Fig. S3*F*) dependent increase in systemic mean arterial blood pressure (sMABP). The increase in sMABP followed the increase in SpV mBF and in mean central venous pressure (mCVP) (Fig. 3*A*). The sMABP returned to baseline values within 60 to 300 s of cessation of stimulation, dependent on the magnitude of the change. Additionally, stimulation also caused an initial transient increase in heart rate (HR, *SI Appendix*, Fig. S3*G*) followed by a decrease, which was variable between animals. The stimulation intensity dependent change of the different physiological parameters at 10 Hz is shown in Fig. 3*B*. A correlation curve between SpA mBF or sMABP versus eCAP amplitude (evoked by stimulation at 10 Hz with bipolar, biphasic symmetric rectangular pulses, 0.4 ms PW, charge range 0 to 20 microcoulombs; µC) is shown in Fig. 3*C*.

Stimulation of isolated SpN fascicles (charge range 0.03 to 1 µC) evoked similar effects, with changes in local and systemic physiological parameters (*SI Appendix*, Fig. S3*H*). In line with stimulation of the entire NVB, these changes were correlated to fascicle engagement (eCAP) but were smaller in magnitude (*SI Appendix*, Fig. S3*I*). No effects on respiration (respiratory rate)

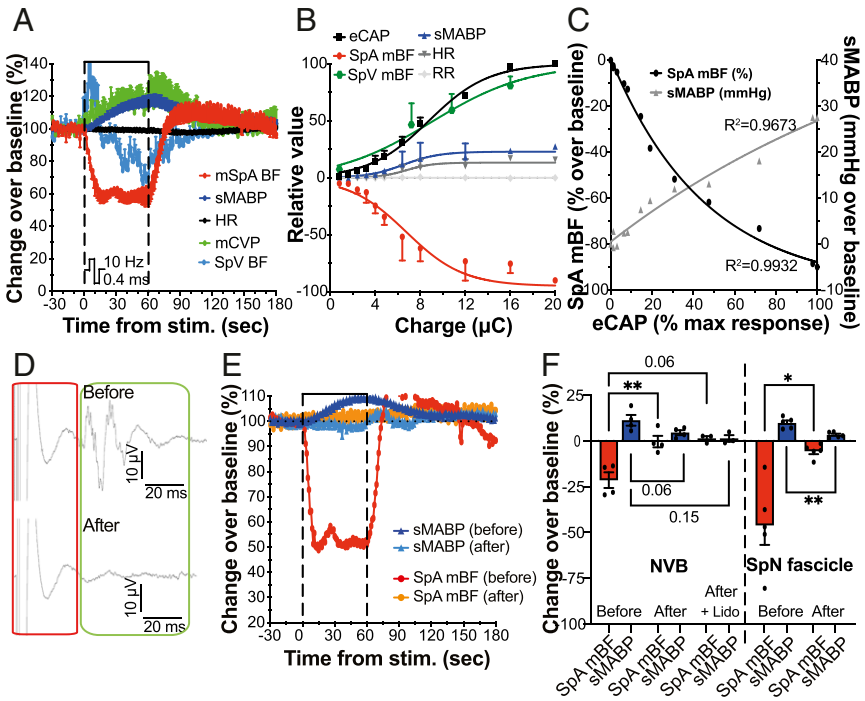

Fig. 3. SpA mBF and sMABP changes are induced by efferent SpN activation and correlate directly with nerve recruitment. (*A*) Effect of splenic NVB stimulation (10 Hz, 0.4 ms PW, and 4.8 µC) on SpA mBF, SpV BF, sMABP, HR, and mCVP. Data are expressed as mean (n = 3) percentage over baseline ± SEM. (*B*) Quantification of the SpN eCAP (expressed as the percentage of the maximum response) and the maximum change (compared to baseline values) in sMABP (mmHg), HR (beat per minute; bpm), SpA mBF (%), and respiratory rate (RR; breaths per min) achieved during stimulation of the pig splenic NVB. Data are shown as mean (n ≥ 4) ± SEM. (*C*) Relationship between eCAP amplitude and SpA mBF (black circles) or sMABP (gray triangles) changes. Data are shown as mean (n ≥ 4). (*D*) Representative eCAP traces of the SpN during NVB stimulation (*Top*) before and (*Bottom*) after nerve transection. Each trace is an average of eight consecutive pulses. (*E*) Relative changes in SpA mBF and sMABP induced by SpNS (isolated SpN fascicle) before and after transection. Data are shown as percentage over baseline from a single representative animal. (*F*) Comparison of the maximum change in SpA mBF (%) and sMABP (%) induced by SpNS before and after transection (for both NVB and isolated fascicle). Data are shown as individual values (n = 4 to 5), with mean ± SEM. All stimulations were applied using bipolar, symmetric, biphasic rectangular pulses at 10 Hz and 0.4 ms PW. *$P \leq 0.05$; **$P \leq 0.01$, or actual P values are shown.

were observed under the conditions tested at any of the stimulation parameter combinations used with either the NVB or isolated fascicles (Fig. 3*B* and *SI Appendix*, Fig. S3*I*).

Importantly, when the fascicles distal to the NVB-stimulating electrode were transected (toward the spleen as shown in *SI Appendix*, Fig. S2*I*) or blocked with lidocaine, the eCAP response was lost (Fig. 3*D*), and the changes in SpA mBF and sMABP (Fig. 3*F*) were abolished. The same phenomenon was observed when stimulating and transecting specific isolated fascicles (Fig. 3 *E* and *F*), thus indicating that SpA mBF and sMABP changes were driven by efferent (toward the spleen), and not afferent (toward the brain), activation of the nerve fascicles.

All together, the data suggest that SpA mBF represents a reproducible nerve-dependent biomarker of SpN engagement across the preclinical species tested.

Stimulation of SpN Releases Noradrenaline that Is Immunomodulatory in Pigs. Toluidine blue-stained semithin sections (*SI Appendix*, Fig. S4 *A* and *B*) did not show evidence of myelination in pig NVB sections. Electron microscopic images of the human NVB showed a similar result: very rare myelinated axons were found interspersed among small unmyelinated axons (*SI Appendix*, Fig. S4 *C* and *D*). Immunohistochemistry analysis confirmed that almost all (>99%) of the neurofilament (NF)/βIII-Tubulin–positive axons of the pig NVB were myelin basic protein (MBP) negative, with very rare MBP-positive axons observed (*SI Appendix*, Fig. S4*E*). Sections of pig VN were used as a control for toluidine blue and MBP staining and showed the expected composition with myelinated and unmyelinated axons (*SI Appendix*, Fig. S5 *A–D*). These results are in line with the electrophysiological experiments and demonstrate that both pig and human SpN are mainly composed of unmyelinated axons.

It is known that the human SpN is composed of sympathetic neurons expressing tyrosine hydroxylase (TH) and lacking choline acetyltransferase (ChAT) (27, 29, 30). We therefore performed staining of the pig NVB for comparison. In line with the human, the pig SpN axons stained positive for TH (*SI Appendix*, Fig. S4*F*), and no ChAT-positive axons were identified. Sections of the VN, known to contain both fiber types, were used as a positive control and showed the expected mixed composition (*SI Appendix*, Fig. S5*C*). Peptidergic neurotransmitters, other than catecholaminergic and cholinergic, are known to play immune modulatory functions. For this reason, we also stained for calcitonin gene-related peptide (CGRP), a well-characterized immune modulatory peptide (31, 32). Only a small proportion (<5%) of the pig SpN axons stained positive for CGRP (*SI Appendix*, Fig. S4*G*), coinciding with recent human data (27). Within the pig spleen, TH-positive axons were again observed and found in close proximity to both CD11b myeloid cells (*SI Appendix*, Fig. S4*H*) and CD3 lymphocytes (*SI Appendix*, Fig. S4*I*) within the marginal zone, red pulp, and periarteriolar lymphoid sheet (*SI Appendix*, Fig. S4 *H* and *I*). Rarely, nerve fibers were observed within the B follicle areas (*SI Appendix*, Fig. S4*J*).

To confirm that SpNS induces release of NA in the pig spleen, we collected blood draining from the spleen (within the SpV) prior to and during two stimulations of the SpN (each delivered for 1 min at 10 Hz, 0.4 ms PW and 4.8 µC, 30 min apart) in

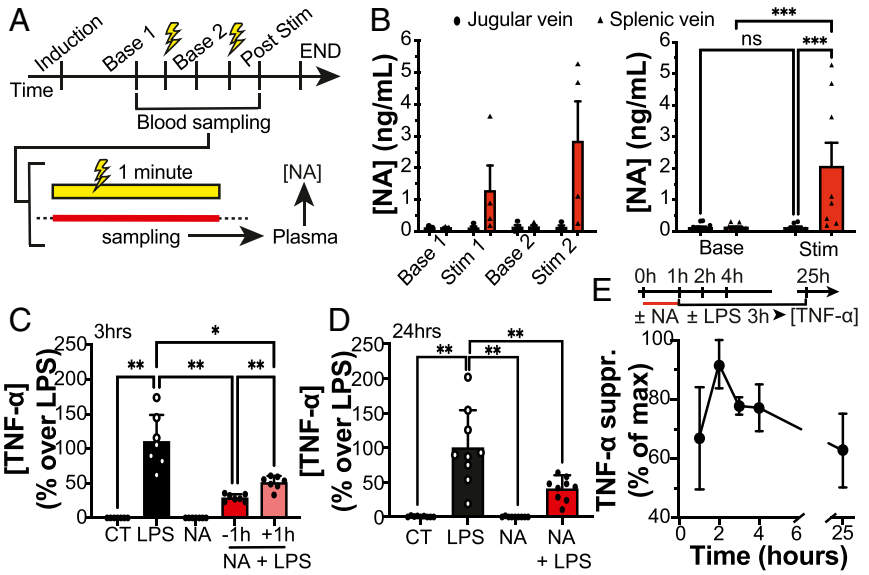

Fig. 4. SpNS releases NA that suppresses TNF-α in pig splenocytes. (*A*) Schematic illustration of the experiments performed to quantify the amount of NA secreted during SpNS in pigs. (*B*) Concentration of NA (ng/mL) found within the SpV and the JV prior (baseline one and baseline two) and during two stimulations (Stim 1 and Stim 2) of the pig splenic NVB. The graph on the right shows the data from both stimulations combined for all four pigs. Individual values (n = 4) with mean + SEM are shown. (*C* and *D*) Quantification of TNF-α concentration in medium conditioned by splenocytes in control (CT; medium only), LPS, NA, or NA + LPS conditions for 3 (*C*) or 24 (*D*) h expressed as percentage over LPS. In *C*, NA was added either 1 h before (−1 h) or 1 h after (+1 h) LPS exposure. Individual values (n = 7 to 9) with mean + SD are shown. (*E*, *Top*) A schematic representation of the experiment in which the optimal time window between NA exposure and LPS challenge was investigated. (*Bottom*) The graph shows the quantification of TNF suppression (expressed as percentage over the maximum response) induced by NA at each time point tested. Data are shown as mean (n = 3) ± SEM $*P \leq 0.05$; $**P \leq 0.01$; $***P \leq 0.001$.

terminally anesthetized pigs (Fig. 4*A*). As a control, we also sampled blood from the jugular vein (JV). While baseline levels (prior to each of the stimulations) of NA were low in both SpV and JV, stimulation induced a significant increase in NA within the SpV only (Fig. 4*B*). Together, these data suggest that catecholamines, such as NA, represent the main neurotransmitter system of the SpN that can carry information to splenic immune cells also in the pig.

Since NA is a key molecular component of the anti-inflammatory reflex in rodents, we utilized NA as a proxy of stimulation and examined its effect on isolated pig splenocytes. Spleens were harvested from pig donors, and total leukocytes were isolated. Cells were then challenged with LPS, with or without NA, and TNF-α concentration in the conditioned medium was quantified. Noradrenaline was able to suppress TNF-α after both 3 h (fig. 4*C*) and 24 h (Fig. 4*D*) of incubation. In addition, NA was able to reduce TNF-α (as measured 3 h post-LPS exposure) when delivered 1 h before or 1 h after LPS exposure, with the former producing a stronger suppression (Fig. 4*C*). We then used this culture system to identify a suitable time window between stimulation (NA) and proinflammatory challenge (LPS) to achieve optimal TNF-α suppression in pigs. Splenocytes were incubated with NA for 1 h prior to being washed and placed into fresh medium. Cells were then challenged with LPS at different times post-NA removal, and TNF-α was measured 3 h post-LPS (Fig. 4*E*). The maximum NA-induced suppression of TNF-α (average ± SD: 37.9 ± 8.3% reduction versus LPS only) was observed when cells were challenged with LPS 2 h from initial NA exposure (Fig. 4*E*).

The above data suggest that the pig SpN releases NA, which is able to suppress TNF-α production by pig splenocytes.

Stimulation of SpN or VN Promotes Immunomodulation in Pigs. In order to assess the translatability of the anti-inflammatory pathway in vivo, we used two acute models of inflammation in pigs. We initially administered a high dose of LPS (2.5 μg/kg; intravenously [i.v.] into the JV) in terminally anesthetized pigs (*SI Appendix*, Fig. S6*A*). In this experiment, we sought to test the protective effect of SpNS in a model in which the complex LPS-induced inflammatory responses are known to cause acute cardiovascular compromise and death within a short time window (33, 34). We used left cervical VNS (LVNS) as a positive control, because of its known protective effects in endotoxemia models, alongside a SpN sham stimulation group (animals receiving the same surgical procedure but no stimulation). In order to select LVNS parameters, we performed preliminary electrophysiology studies and selected a stimulation amplitude able to activate all fiber types contained within the cervical VN (*SI Appendix*, Fig. S5 *E–I*), including small myelinated and unmyelinated axons that are reported to be the main constituent of the abdominal portion of the VN in pigs and humans (15).

Stimulation of the SpN (or LVN) was delivered 3 h prior to LPS challenge and at the time of LPS injection (1 min stimulation at 10 Hz both times). Target engagement in the SpNS group was confirmed by a reduction in SpA mBF of (average ± SD) 37.41 ± 18.73% (*SI Appendix*, Fig. S7), corresponding to ∼25% eCAP activation (range 10 to 50%). Target engagement in the LVNS group was confirmed by the presence of VNS-induced changes in physiology: bradycardia, hypotension, and bradypnea (*SI Appendix*, Fig. S5*J*). Before and after the first stimulation (or sham) period (and prior to LPS in vivo injection), peripheral whole blood was collected longitudinally to assess systemic immunomodulatory/suppressive effects of SpNS or LVNS using an ex vivo LPS-induced challenge. No differences between groups were observed in the ex vivo LPS-induced TNF-α levels up to 2 h poststimulation (*SI Appendix*, Fig. S6*B*). Additionally, no significant differences in peripheral total white blood cell count (*SI Appendix*, Fig. S6*C*) or other hematological parameters (*SI Appendix*, Table S2) were observed between groups. Only time-dependent effects were observed in all groups and likely related to the procedure (surgery and anesthesia) per se. No significant changes over time were observed in biochemical

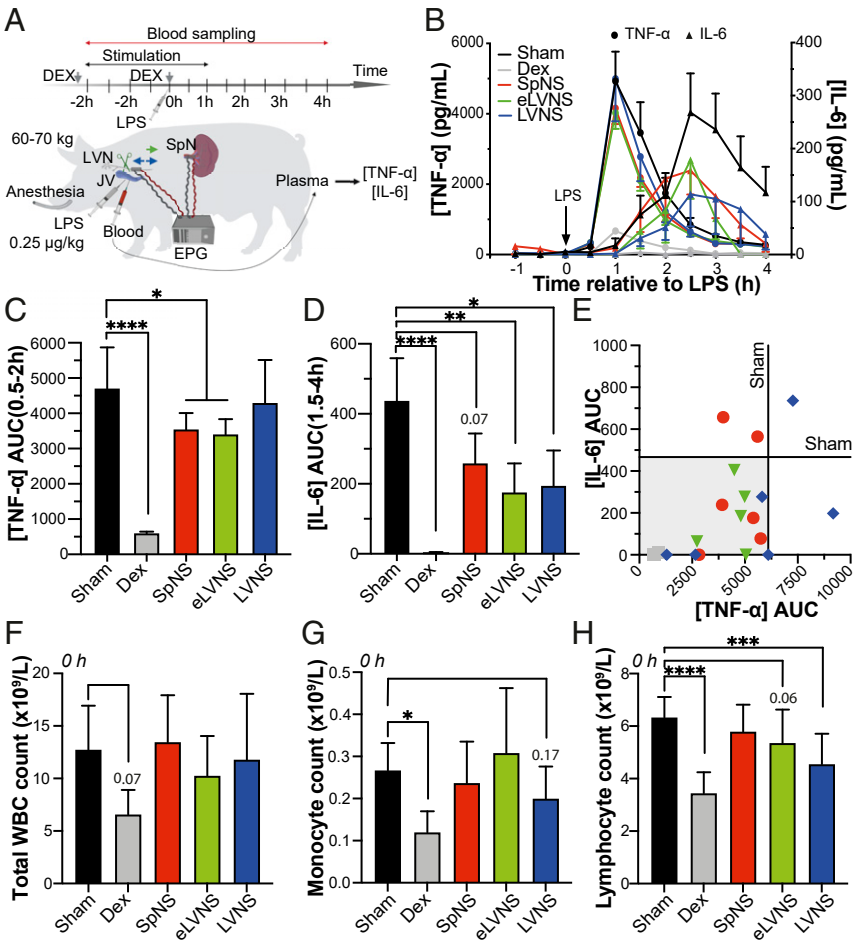

Fig. 5. SpNS and eLVNS reduces TNF-α and IL-6 in a low-dose LPS model. (*A*) Schematic illustration of the low-dose (0.25 µg/kg, i.v.) LPS model in pigs. Animals were divided into five groups (sham, n = 7, black; dexamethasone, n = 3, gray; SpNS, n = 6, red; LVNS, n = 6, blue; eLVNS, n = 5, green). Dexamethasone (Dex) was administered immediately after induction of anesthesia (−2.5 h) and at the time of LPS injection (0 h). Electrical stimulation was delivered continuously from −2 to 1 h relative to LPS injection. Blood samples were collected every 0.5 h, between −2 and 4 h, from the JV for cytokine as well as for hematology and biochemistry analysis. (*B*) Concentration (pg/mL) of TNF-α (circles; left *y*-axis) and IL-6 (triangles; right *y*-axis) over time in all groups. Data are shown as mean (n = 3 to 7) ± SEM. (*C* and *D*) Quantification of total cytokine production as measured by AUC between (*C*) 0.5 to 2 h post-LPS for TNF-α and between (*D*) 1.5 to 4 h for IL-6. Data are shown as mean (n = 3 to 7) + SD. (*E*) Concentration of TNF-α and IL-6 (expressed as AUC) for each individual animal within the four treatment groups. The solid lines indicate the mean TNF-α and IL-6 AUC values of the sham group. The bottom left quadrant in gray indicates the area in which therapeutic efficacy (concomitant reduction of TNF-α and IL-6 versus mean sham values) is achieved. (*F–H*) Quantification of peripheral blood white cell count in the different groups; specifically, (*F*) total white blood cells, (*G*) monocytes, and (*H*) lymphocytes measured at time 0 h (prior to LPS injection). Data are shown as mean (n= 3 ot 7) + SEM. *$P \leq 0.05$; **$P \leq 0.01$; ***$P \leq 0.001$; ****$P \leq 0.0001$, or actual *P* values are shown.

parameters including pancreatic and renal enzymes (*SI Appendix*, Table S3).

Following LPS injection, leukopenia and hypotension were observed at 0.5 h post-LPS in the sham animals (*SI Appendix*, Fig. S6 *C* and *D*). Hypotension normally developed within 10 min following injection, rapidly reaching sMABP values of 40 mmHg (*SI Appendix*, Fig. S6*D*), accompanied by tachycardia and/or tachyarrhythmia (five out of six; *SI Appendix*, Table S4), requiring the use of vasopressin (six out of six; *SI Appendix*, Fig. S6 *D* and *E*) and antiarrhythmic drugs (*SI Appendix*, Table S4). The sMABP dropped to about 60% below the pre-LPS baseline in most sham animals 30 min after LPS injection (*SI Appendix*, Fig. S6*F*). Stimulated animals, while still showing leukopenia (*SI Appendix*, Fig. S6*C*), did not show extensive reduction in sMABP (*SI Appendix*, Fig. S6*E*), and only a few animals displayed tachycardia and/or tachyarrhythmia (one out of six; *SI Appendix*, Table S4) or required vasopressin (two out of six SpNS and one out of six LVNS; *SI Appendix*, Fig. S6*F*). Animals that reached an sMABP of less than 40 mmHg, despite pharmacological treatment, were euthanized (*Materials and Methods*). Euthanasia had to be induced in 83.3% (five out of six) of sham animals within 2 h post-LPS, but only in 16.6% (one out of six) of animals in either the SpNS or LVNS groups (*SI Appendix*, Fig. S6*G*). Since sham animals required multiple pharmacological treatments within the first 0.5 h and some animals reached the humane endpoint before this time point, a comparison of cytokine levels (between treated and sham animal) was not possible in this model. However, TNF-α and interleukin 6 (IL-6) levels were partially increased (versus baseline) at 0.5 h in all groups, and both SpNS and LVNS animals showed similar trends in cytokine profiles over the course of 2 h post-LPS injection (*SI Appendix*, Fig. S6*H*). Quantification of the area under the curve (AUC) between 0 and 2 h post-LPS (for both TNF-α and IL-6) showed no difference between SpNS and LVNS groups (*SI Appendix*, Fig. S6 *I* and *J*).

These data indicated that SpNS and LVNS had similar protective effects in a model involving cardiovascular compromise caused by LPS.

Successively, we used a low-dose LPS model (0.25 μg/kg of LPS, i.v.) in order to accurately assess the effect of SpNS on cytokine production (Fig. 5*A*). This LPS dose induced cytokine production and hematological changes, without severe cardiovascular effects, in line with previous literature (35). In addition to sham, SpNS, and LVNS, an additional group of animals received i.v. injections of dexamethasone (0.5 mg/kg; 2.5 h before and at the same time of LPS injection) as a positive control for cytokine suppression, and a further group received stimulation of the efferent trunk of the LVN (eLVNS) in order to activate peripheral connections only (Fig. 5*A*). In order to maximize the effect, SpNS, LVNS, and eLVNS were delivered for a longer time (from −2 h to +1 h relative to LPS injection) and at 1 Hz, instead of 10 Hz, to reduce stimulation-induced cardiovascular changes. The charge used for SpNS, LVNS, and eLVNS was in line with the previous experiment.

After LPS injection, there was initial leukopenia with reduction in circulating neutrophils, monocytes, and lymphocytes followed by the leukocytosis with an increase in circulating neutrophils in all groups. Circulating levels of monocytes and lymphocytes, instead, remained low until the end of the observation period (4 h after LPS) (*SI Appendix*, Fig. S8 *A–D*). A statistically significant ($P < 0.01$) effect of time on total white blood cell count as well as lymphocyte, monocyte, and neutrophil counts was observed in all groups. Dexamethasone showed the smallest changes in leukocyte counts versus baseline (0 h) levels. In parallel to hematological changes, LPS caused a dynamic accumulation and clearance of peripheral TNF-α and IL-6 (Fig. 5*B*) reaching maximum at 1 h and 3 h post-LPS, respectively. Dexamethasone caused suppression of LPS-induced TNF-α and IL-6 (Fig. 5 *B–D*) compared to sham animals. Importantly, all electrically stimulated groups displayed partial cytokine suppression (Fig. 5 *B–D*). Interestingly, SpNS and eLVNS both resulted in a similar reduction (versus sham) in TNF-α and IL-6 measured as AUC (Fig. 5 *C* and *D*). Conversely, LVNS animals showed a highly variable response in TNF-α reduction (Fig. 5*C*) but a more reproducible reduction in IL-6 (Fig. 5*D*). When looking at each individual animal and the relative concentration of TNF-α and IL-6 (vs. sham animals), SpNS had a global modulatory effect (gray box in Fig. 5*E*) in 66.6% of animals (four out of six); for the VN groups, eLVNS had global modulatory effects in 100% of animals (five out of five), while LVNS had effects in 50% (three out of six animals) (Fig. 5*E*). Dexamethasone showed a modulatory effect in all three animals. Of note was the finding that the suppression of TNF-α and IL-6 induced by dexamethasone occurred in combination with a significant reduction of circulating leukocytes (Fig. 5*F*), mainly driven by a reduction in monocytes (Fig. 5*G*) and lymphocytes (Fig. 5*H*), within 2.5 h after administration of a single dose (0 h; prior to LPS administration). However, no significant changes in peripheral leukocyte counts (as measured prior to LPS injection) were observed either in SpNS or eLVNS groups (Fig. 5 *F–H*). A small but statistically significant reduction of circulating numbers of lymphocytes was observed in the LVNS group (Fig. 5*H*).

These data indicated that SpNS was able to reduce LPS-induced systemic cytokine production. This effect was reproduced by eLVNS, which showed a superior effect compared to LVNS.

Discussion

Herein, we have shown that the pig represents a good model of the human splenic innervation. The similarity in dimensions (artery size), anatomy (single artery; periarterial nerves only), and histological properties (number of fascicles; unmyelinated, catecholaminergic axons) allows for a more refined preclinical assessment of stimulation requirements of the human SpN. In such a model, we showed that immune responses can be regulated by stimulating the splenic or the VN in line with previous rodent work (4, 7, 24). Activation of splenic circuits via near-organ stimulation of the SpN caused a 20 to 30% reduction in circulating levels of TNF-α and a 40 to 50% reduction in IL-6 following a low-dose LPS challenge. Corroborating this finding, we observed that stimulation of the eLVN led to a similar suppression profile, while stimulation of the intact LVN did not result in a clear TNF-α reduction in this setting. A recent study in rats showed very similar results: stimulation of the intact LVN in anesthetized rats resulted in a highly variable response in TNF-α suppression, while eLVNS had a significantly more consistent effect (20). The reason for this is not yet understood and may be related to different effects of afferent and efferent pathways (22) activated in the VN by electrical stimulation, especially under anesthesia when central mechanisms (i.e., via the brain) may be affected. These data suggest that neurotransmitter release induced by SpNS or VNS regulates cytokine production following LPS injection. Importantly, the similar profile of SpNS and eLVNS supports the evidence that anti-inflammatory mechanisms are regulated in abdominal organs, mainly the spleen, in pigs. This is in line with the anti-inflammatory pathway described in rodents (3, 4, 6).

Here, we propose that NA may represent a key molecular mediator of the anti-inflammatory mechanisms also in the pig spleen. We have shown that the SpN in pigs, in line with humans (27, 29, 30), is catecholaminergic (TH-positive) in nature and releases NA upon stimulation. Our in vitro splenocyte model demonstrated that NA is a fundamental mediator of TNF-α regulation in pigs, thus potentially linking it to the in vivo immunomodulatory results. The key importance of NA and its receptors expressed by immune cells within the spleen is in line with previously published literature in rodent models. Preliminary data from our group shows that NA acts on pig splenic myeloid cells via beta adrenergic receptors to modulate cytokine production. These data looking at the translation of the molecular mechanism of the anti-inflammatory reflex across species are currently being published separately.

Interestingly, we have also potentially identified effects associated with SpNS and LVNS beyond modulation of cytokines. Electrical stimulation prevented cardiovascular collapse in our pig high dose LPS model, prior to cytokine flare. Since cardiovascular collapse occurred in sham animals prior to the time points at which cytokines reach significant up-regulation (1 h post-LPS for TNF-α; 2 h post-LPS for IL-6), the different cardiovascular response in stimulated animals could not be explained by cytokine modulation. Furthermore, although LVNS did not result in clear TNF-α modulation in the low-dose LPS model, it did have a protective effect in the high dose model, similar to SpNS. This effect has also been observed previously in a different sepsis model in pigs in which VNS induced cardiovascular protection in the absence of cytokine modulation (36). Combined, these results suggest that SpNS and VNS may have broader immune regulatory effects. The exact mechanism and mediators able to explain this substantial effect remains to be clarified. Prevention of cardiovascular collapse in pigs has been previously shown in a very similar model in which the treatment of pigs with diclofenac sodium prior to LPS injection promoted cardiovascular stability and improved survival without significant effects on cytokines (33). This effect was related to the suppression of lipid mediators, in particular inflammatory eicosanoids. Interestingly, vagotomy has been shown to delay resolution of experimental infection in mice by impacting lipid mediator production (37). Therefore, it is possible that vagal and splenic fibers may be regulating mediators important for inflammation resolution and cardiovascular protection. Indeed, we have shown that SpNS in implanted conscious pigs increased the concentration of specialized proresolving mediators in peripheral plasma of stimulated animals, with a concomitant reduction of proinflammatory eicosanoids including prostaglandin (38). However, further studies are being conducted to better understand the broad spectrum of mechanisms associated with SpNS.

We have shown by immunohistochemistry and electrophysiology that across the investigated species, the SpN is a periarterial plexus characterized by absence of myelin and low conduction velocities, typical of unmyelinated axons (39, 40). This characteristic drives the need of high charge requirements as compared to stimulating myelinated nerves. However, electrophysiology characterization also demonstrated that the rat NVB has a two order of magnitude smaller charge requirement as compared to pigs and humans. Due to similarities in anatomy and fascicle composition, the charge requirements for stimulation of the mouse NVB are expected to be close to those of the rat. This difference between rodents and large animals is an important concept in device development since parameters for human target (i.e., nerve) engagement have to be accurately determined in order to drive the user requirements (e.g., charge capabilities, charge injection limits) of the active implantable medical device (i.e., electrodes and implantable pulse generator). In addition, the number of fascicles, their dimension and distribution as well as the anatomy of the SpA underpinned the superiority of the pig as a model of the human splenic anatomy. The ability to access longitudinal portions of the splenic NVB for interface implantation makes the pig a robust and relevant preclinical model for designing and validating clinical implantable devices for SpNS to modulate inflammation. Although rodent disease models are extremely valuable for biological proof of concept and elucidation of mechanisms, inherent anatomical and functional differences can limit their use for the development of clinical bioelectronic medicines. Large animal models can therefore bridge this gap to bring bioelectronic medicine development closer to human translation.

The higher charge requirement for up to 50% nerve recruitment observed in the human samples versus the pig is likely due to a larger proportion of interspersed adipose and connective tissue observed in the human versus the porcine NVB. The human tissues were collected from a wide demographic, contrary to the research animals, which were lean and young individuals of similar body weights and age. For full nerve recruitment, however, charge requirements were similar between the pigs and the human samples, most likely because the porcine SpN contains almost twice the number of axons and consequently requires greater charge for full activation. However, some of these differences may be also influenced by technical discrepancies (e.g., ex vivo versus in vivo, tissue temperature, type of electrodes).

Of note was the observation that immunomodulatory effects of SpNS were achieved with submaximal stimulation and were comparable to that achieved with stimulation of the VN. All of these observations are important considerations when refining stimulation parameters in preclinical models and predicting energy requirements prior to clinical use. As we have recently shown, in silico modeling and ex vivo human studies can help to further determine boundary variables, such as tissue impedance and conductivity of adipose/connective tissue constituents of the target structure, to refine power requirements and determine the expected variability of clinical parameters (12). Ultimately, chronic large animal studies (38) and clinical trials (both acute and chronic) will finalize the requirements for stimulation in order to achieve therapeutic effects.

The local physiological responses to SpNS, such as change in SpA BF, may be valuable as an indicative biomarker of SpN engagement. The correlation between SpN recruitment and SpA flow was particularly useful. Although SpN-induced changes in local blood flow were previously reported in large animal species (41, 42), our work represents an in-depth characterization of this physiology and relationship to nerve activation. During 1 min of stimulation at 10 Hz, the maximum reduction in SpA mBF corresponded to the maximum recorded eCAP in anesthetized pigs. Reduction in SpA mBF could therefore be used as a real-time dose–response biomarker for nerve engagement during surgical implantation of the bioelectronic device and for patient-specific determination of the range of stimulation parameters. In support of this notion, ex vivo data from others have shown that SpA BF is reduced during stimulation of human SpN (43). Further translational data will be gathered in clinical studies, such as those recently initiated to demonstrate feasibility and safety of acute SpNS (https://www.clinicaltrials.gov identifier NCT04171011).

The observed systemic physiological responses to SpNS in the pig, namely transient mild increases in sMABP and HR, are explained by an increase in venous return (due to splenic contraction) and resultant positive chronotropy and vasoconstriction in line with previous observations in other species including cats and dogs (44, 45). In our study, stimulation of the SpN in the pig was consistently associated with splenic contraction, increased SpV blood flow, and an increase in mCVP that preceded the rise in sMABP. Splenic contraction is driven by smooth muscle activation and likely related to the central baroreflex as previously described in dogs (45). While ex vivo and in vivo human studies have shown contradictory results on the capacity of the spleen to contract (43, 46), clinical studies will help to understand if SpNS causes contraction-related or -unrelated systemic effects in humans. While acutely these changes may be tolerable and useful for target engagement definition, for chronic applications, potential systemic effects should preferably be limited. We have recently performed electrophysiology studies to identify stimulation parameters able to minimize splenic contraction-induced cardiovascular effects while maintaining neurotransmitter release sufficient to modulate immune responses in pigs (38).

We have observed very few CGRP-positive axons and no clear afferent pathway-related physiological effects in our acute anesthetized pig studies. This is in line with previous literature in stating the absence of afferents in nonhollow organs like the spleen (47). There is, however, some contention (e.g., in dog studies) suggesting the existence of afferent pathways associated to mechanical and pressure responses (48) and potentially relaying inflammatory status (49). However, chronic conscious pig studies are best placed to address the presence or absence of systemic afferent circuit-mediated behavioral responses. Data recently collected from such studies, that we have published elsewhere (38), suggest that stimulation is well tolerated in conscious pigs.

Importantly for clinical translation, hematological analysis showed that neither a short (1 min) nor prolonged (2 h) acute SpNS caused systemic immune-suppressive responses as indicated by the numbers of circulating leukocytes as well as by the ex vivo LPS assay. This was also observed for eLVNS and partially with LVNS. However, SpNS and eLVNS had a very different profile in comparison to pharmacological treatment with dexamethasone, which promoted a substantial reduction in cytokine levels at the expense of systemic immune suppression (i.e., reduction of circulating levels of leukocytes). This suggests that neuromodulation may provide some beneficial therapeutic effect without causing significant suppression of systemic immune defenses.

The splenic NVB is located in close anatomical proximity to the pancreas and the left kidney. However, when compared to sham and VN implanted pigs, implantation and simulation of the SpN did not acutely affect organ function as assessed by biochemical analysis of pancreatic and kidney enzymes. However, chronic studies will help to further determine the effect of chronic implantation and daily stimulation of the SpN on hematological and biochemical parameters in animals and humans.

Finally, this study also highlights the need for further investigation of which subset of fibers within the VN are required to drive the anti-inflammatory effect. The pig has been proposed as an appropriate model for assessing and refining VNS parameters (21) due to the anatomical and physiological similarities between

the pig and human VN. In both species, unmyelinated and small myelinated fibers carry signals to and from abdominal organs (15). This suggests that the activation of unmyelinated and small myelinated fibers within the cervical VN may be required to maximally activate efferent connections to the spleen as demonstrated in rodents (8). To achieve this, stimulation charges to activate these fibers (as used here) would be higher in comparison to those normally used in the clinic (14, 21, 50). Therefore, stimulation at the required intensity would also activate multiple motor and additional autonomic pathways with resultant off-target effects. These levels of stimulation are unlikely to be reached in patients due to intolerance of off-target effects (21). Additional validation and optimization of stimulation parameters and/or neural interfaces may therefore be needed to achieve even greater immunomodulatory responses (14) while reducing off-target effects in patients subjected to VNS. Conversely, if a different pathway for immunomodulation exists (e.g., via low threshold efferent/afferent myelinated fibers within the VN), acute electrophysiology studies and chronic efficacy studies in translational species could also allow identification of fiber types and parameters resulting in modulatory effects translatable to clinical use.

The data presented here provide a demonstration of the existence of anti-inflammatory circuits in a large and clinically appropriate translational species such as the pig. Importantly, we have refined a pig inflammatory model (low-dose LPS challenge in adult pigs) that can be leveraged for future neuroimmune modulation studies. Furthermore, we show a clear immunomodulatory therapy opportunity by targeting near-organ nerves associated with the spleen and confirming target engagement through physiological, neurological, and immunological readouts. The use of human tissues and large animals has enabled the development of a suitable model for SpN bioelectronic medicine development as well as provided a dataset fundamental for the translation of near-organ neuromodulation of the immune system into human clinical trials.

Materials and Methods

All animal studies were ethically reviewed and carried out in accordance with Animals (Scientific Procedures) Act 1986. The protocol was approved by the Royal Veterinary College Animal Welfare and Ethical Review Board and the Galvani Bioelectronics Animal and Scientific Review Committee. All animals were transported and housed under conditions specified in the UK Animal Welfare Act 2006 and The Welfare of Farm Animals (England) Regulations 2007. Human tissues were obtained from deceased human pancreas donors in which the pancreas was deemed unsuitable for transplantation. Informed consent for the use of the human tissue for this project was provided by the donors' families. Ethical approval for the studies was obtained from National Research Ethics Service Committee East of England—Cambridge South (Research Ethics Committee Reference 16/EE/0227).

Cadaveric Porcine Gross Anatomy. To identify an animal model of relevant splenic neurovascular anatomy and size, which could serve as a human translational model, cadaveric dissections were performed in 12 farm pigs of various body weights (female; Large White/British Landrace cross; body weight 22 to 110 kg). SpA dimensions and spatial relationships to adjoining structures such as the SpV were recorded, and accessible locations for splenic NVB interface implantation, enabling dissection and implantation with minimum risk of causing iatrogenic damage to the SpN plexus, were investigated based on the experience of the veterinary surgeon in attendance.

Acute Terminal Anesthetized Experiments—Pigs. A total of 62 farm pigs (female; Large White/British Landrace cross) were sourced from a commercial pig farm and acclimatized at the research facility for a minimum of 7 d prior to the experiment; animals were used for electrophysiological studies (n = 6, body weight 45 to 55 kg, age 10 to 12 wk), high dose LPS models (n = 18; body weight 45 to 55 kg, age 10 to 12 wk), low-dose LPS models (n = 27; body weight 60 to 70 kg, age 12 to 14 wk), and in vitro splenocytes experiments (n = 7; body weight 60 to 70 kg, age 12 to 14 wk). Four Berkshire pigs (body weight 60 to 70 kg, age 12 to 14 wk) were used for in vivo NA measurement experiments.

Electrophysiology Experiments—Pigs. Animal handling and management, anesthesia protocol, and surgical approach on the day of the experiment is described in *SI Appendix*. In brief, commencing at the origin of the SpA, a 10 mm long segment of the artery with an intact periarterial SpN plexus was carefully separated from the SpV and surrounding loose connective tissue. This splenic NVB was subsequently instrumented with a bipolar circumferential cuff electrode (2.5 mm diameter, 8 mm length; cathode surface area: 0.13 cm^2; #1041.2180.01, CorTec GmbH). Distal (ca. 1 to 2 cm) to this site a minimum of one discrete SpN fascicle was carefully isolated and subsequently instrumented with one cuff electrode (diameter 0.5 mm, length 5.5 mm; cathode surface area: 0.0063 to 0.01 cm^2; #1041.2115.01 or #1041.2112.01; CorTec GmbH). At the level of the splenic hilum (ca. 5 to 6 cm from NVB cuff), a minimum of one discrete SpN fascicle was carefully isolated and instrumented with one cuff electrode (diameter 0.5 mm, length 5.5 mm; cathode surface area: 0.0063 to 0.01 cm^2; #1041.2115.01 or #1041.2112.01; CorTec GmbH) to record eCAP. For monitoring blood flow changes during SpNS, an ultrasonic transit time flow probe (Transonic Systems, Inc.) was placed around the SpA immediately proximal to the branching of the left gastroepiploic artery from the SpA and around the SpV at the level in which the vessel exited the spleen at the hilum. Flow changes were continuously monitored via a TS420 perivascular flow module (Transonic Systems, Inc.), and measurements were digitally recorded using a 16 channel PowerLab acquisition system (ADInstruments) with LabChart 8 software at 2 kHz sampling frequency. The stimulation parameters used and the details of the analysis are reported in *SI Appendix*.

NA In Vivo Measurements—Pigs. Animal handling, management, anesthesia protocol, and surgical procedure were as above. In addition, after cuff implantation, a catheter was inserted into the SpV and routed toward the base of the spleen. Animals were then allowed to stabilize for 30 min. Blood (5 mL) was collected simultaneously from the SpV and the JV over 60 s. Splenic NVB stimulation (Stim 1) was performed 10 min later for 1 min at 10 Hz (bipolar, symmetrical biphasic rectangular pulses), and blood was collected as before. After 30 min, blood sampling was performed again during another baseline (Baseline 2) and stimulation (Stim 2) procedure. A sham (no current applied) stimulation was used as control. Samples were transferred immediately to ethylenediaminetetraacetic acid (EDTA) vacutainers, mixed by inversion, and stored on ice. Plasma was isolated by centrifugation (2,000 × *g* for 5 min), added to stabilizing solutions (as per enzyme-linked immunosorbent assay [ELISA] instructions), and immediately frozen on dry ice. Frozen plasma aliquots were thawed and immediately analyzed by ELISA for quantification of NA using the Noradrenaline Sensitive ELISA (DLD Diagnostika, category no. ea633/96) according to manufacturer's instructions. Plates were analyzed using the Infinite 200 PRO spectrophotometer and iControl software (Tecan Group Ltd.).

Pig Splenocyte Experiments. General anesthesia, maintenance, and surgical procedure were performed as described above. The major vessels (splenic, short gastric, and gastroepiploic arteries and veins) were sequentially ligated, and the vessels were transected. The omentum was incised, and the spleen was removed. Animals were then euthanized by barbiturate overdose. Spleens were cut into four sections, and 5 g of tissue was sampled from the middle of each section, rinsed in cold phosphate-buffered saline (10204733, Fisher Scientific), and passed through a metal strainer under gentle manual pressure using a 50 mL syringe plunger. Total leukocytes were then extracted to perform challenge experiments. Details can be found in *SI Appendix*.

High-Dose LPS Model—Pigs. Animal handling, management, and anesthesia protocol on the day of the experiment was identical to that described above, and the experiment setup is illustrated in *SI Appendix*, Fig. S6*A*. Animals were randomly divided into three treatment groups with six animals per group, receiving either stimulation of the SpN (SpNS group; instrumented with a NVB cuff electrode and a SpA flow probe as described above), LVNS, or no stimulation (sham group). Animals in the LVNS group were placed in dorsal recumbency, and the left ventral neck was clipped, aseptically prepared, and draped in a routine fashion. Using aseptic technique, a 10 cm longitudinal skin incision was placed immediately to the left of the trachea from the larynx caudad. The incision was continued through the subcutaneous tissue and the sternohyoideus muscle until encountering the carotid sheath and left VN. A 1 cm segment of the LVN was circumferentially isolated from surrounding loose connective tissue by careful blunt dissection and was subsequently instrumented with a bipolar circumferential cuff electrode (2.0 mm diameter, 8 mm length; cathode surface area: 0.05 cm^2; #1041.2179.01, CorTec GmbH). Sham group animals received the same

surgical approach as the SpNS group and were instrumented with a SpA flow probe as described above; however, no NVB cuff electrode was implanted. In this group, the SpA was manually occluded for 1 min, achieving ~50% flow reduction at the two stimulation time points, mimicking the SpA flow reduction evoked by SpNS. Animals were injected i.v. into the JV with 2.5 μg/kg body weight of LPS 3 h after initial stimulation (purified LPS from the cell membrane of *Escherichia coli* O111:B4; Sigma-Aldrich). Following LPS administration, animals were euthanized with an overdose of pentobarbital (administered i.v.) when the sMABP reached levels below 40 mmHg despite pharmacological treatment (defined as the humane endpoint) or when the animal completed the predetermined study time window of 2 h post-LPS injection. All of the details regarding stimulation parameters, blood sampling, LPS dosing, and pharmacological treatment are reported in *SI Appendix*.

Low-Dose LPS Model—Pigs. Animal handling, management, and anesthesia protocol on the day of the experiment was identical to that described above, and the experiment setup is illustrated in Fig. 5*A*. Animals were randomly divided into five treatment groups: sham (n = 7), SpNS (n = 6), LVNS (n = 6), eLVNS (n = 5), and dexamethasone (Dex) (n = 3). Animals within the Dex group received two i.v. boluses of dexamethasone (0.5 mg/kg each) after induction of anesthesia (2.5 h prior to LPS injection) and at the time of LPS injection. Animals within the Dex group were maintained under general anesthesia for the same duration as the other animals, but no surgical procedure, apart for instrumentation (central vein and arterial catheters), was performed on these animals. The animals within the other groups were subjected to surgical procedures. The SpNS and sham group received a laparotomy (as described above), and a transit time flow probe was placed on the distal SpA. The SpNS group was also implanted on the proximal/middle NVB with a cuff electrode (5 mm diameter, 10 mm long spiral cuff electrode, CorTec GmbH). The LVN was accessed in animals belonging to LVNS and eLVNS groups. The VN was accessed as described above and implanted with a 2 mm cuff electrode (2.0 mm diameter, 8 mm length; cathode surface area: 0.05 cm^2; #1041.2179.01, CorTec GmbH). After cuff implantation, the LVN was ligated just proximal to the cuff and then cut to eliminate central connections in the eLVNS group.

Electrical stimulation was delivered continuously for 3 h (−2 to +1 h relative to LPS injection) at 1 Hz; low-frequency stimulation was chosen in order to prevent cardiovascular effects during the prolonged stimulation duration. The amplitude of the stimulation was such to recruit ~10 to 50% of the SpN axons and myelinated and unmyelinated axons of LVN. LPS (0.25 μg/kg; *E. coli* O111:B4; Sigma-Aldrich) was injected i.v. (via the JV) 2 h from the initiation of the stimulation. The LPS was prepared in sterile saline and then diluted in injectable saline (0.5 mL LPS solution in 9.5 mL saline) to achieve the right concentration and administered over a period of 5 min (2 mL/min). Peripheral blood samples were collected every 0.5 h from −1 h to +4 h (relative to the LPS injection time point) in plain and EDTA tubes for hematology and clinical biochemistry. Additional EDTA samples were centrifuged at 2,000 × *g* for 5 min at 4 °C. Plasma was separated and frozen on dry ice and stored at −80 °C prior to TNF-α and IL-6 quantification using commercially available ELISA kits (Porcine TNF-alpha; DY690B, and porcine IL-6, DY686; DuoSet Solid Phase Sandwich ELISA, R&D Systems).

Rat Experiments. Four female Lewis rats (150 to 200 g, sourced from Charles River) were acclimatized at the research facility for 7 d prior to experiments. Rats were group housed and given ad libitum access to food and water during the acclimatization period. On the experimental day, anesthesia was induced and maintained with isoflurane vaporized in 100% oxygen with a fresh gas flow of 1.5 L/min. Animals were placed in dorsal recumbency, and the ventral abdomen was clipped and aseptically prepared and draped in a routine fashion. The spleen was accessed by performing a ventral midline laparotomy using aseptic technique, and gross anatomical features such as SpA dimensions were recorded prior to instrumentation for the electrophysiological experiment as detailed below. After the completion of each experiment, animals were euthanized by administering an overdose of pentobarbital i.v., after which the spleen with intact neurovasculature was rapidly harvested and fixed in 10% neutral buffered formalin for histological analysis.

Electrophysiological Experiments—Rats. Animal handling, management, and anesthesia protocol on the day of the experiment is described above. The splenic NVB was isolated at the common SpA level by blunt tissue dissection and instrumented with a bipolar circumferential cuff electrode (0.4 mm diameter, 3 mm length; CorTec GmbH). Approximately 1 cm distal to this periarterial cuff electrode, some of the fascicles were carefully separated from the artery and placed onto silver chloride hook electrodes to record eCAPs as detailed in *SI Appendix*.

Neurovascular Bundle Histology. The NVB from the different species was collected and sectioned at different levels. All samples (mouse/rat: n = 4; pig: n = 6, 45 to 55 kg and n = 6, 70 to 110 kg; human: n = 6) were collected postmortem and immediately fixed in 10% formalin. All segments were paraffin embedded, and 4 to 5 μm thick sections were obtained and stained with Hematoxylin and Eosin. Further details can be found in *SI Appendix*. Images of the sections were then captured with a microscope at 2 to 20× magnification and analyzed with ImageJ software. In these images, the external SpA diameter was measured, and every SpN fascicle was identified and manually selected by using the ImageJ Region of Interest Manager function. The number of SpN fascicles were counted, and the fascicle sizes were assessed by measuring minimum Feret's diameter (μm). The distance of each nerve fascicle from the external arterial wall was measured by drawing the shortest possible perpendicular line from the perimeter of each fascicle to the outer arterial wall. SpA external diameters were also measured.

Human Splenic Nerve Electrophysiology. Specimens containing the splenic NVB, SpV, part of the pancreas and spleen were collected postmortem from organ donors. Samples were immediately placed in cold University of Wisconsin organ preservation solution and placed on ice for transportation. Once into the laboratory, the samples were placed in a Petri dish, and the NVB was then carefully surgically isolated from excess adipose tissue and the SpV. Stimulation and recording were performed as previously described (12) and summarized in *SI Appendix*. More extensive data and analysis on human samples for in silico modeling validation were recently published elsewhere (12).

Statistical Analyses. Statistical significance was defined as $P \leq 0.05$, and analyses were performed with commercially available statistical software (JMP Pro-13.0.0 and GraphPad Prism 9.0) using Student's *t* test or ANOVA analysis. Details can be found in *SI Appendix*.

Data Availability. All study data are included in the article and/or *SI Appendix*.

ACKNOWLEDGMENTS. We thank Dr. Kourosh Saeb-Parsy and Nikola Dolezalova at Addenbrooke's Hospital (Cambridge, United Kingdom) for dissecting human tissues and Sarah Hassan for providing mouse and rat tissues for histology. We are also grateful for the generous donation of postmortem human tissues. We acknowledge the use of https://BioRender.com for the generation of schematics and graphics contained in the manuscript figures.

1. G. P. Chrousos, The hypothalamic-pituitary-adrenal axis and immune-mediated inflammation. *N. Engl. J. Med.* **332**, 1351–1362 (1995).
2. S. S. Chavan, K. J. Tracey, Essential neuroscience in immunology. *J. Immunol.* **198**, 3389–3397 (2017).
3. K. J. Tracey, The inflammatory reflex. *Nature* **420**, 853–859 (2002).
4. L. V. Borovikova *et al.*, Vagus nerve stimulation attenuates the systemic inflammatory response to endotoxin. *Nature* **405**, 458–462 (2000).
5. J. M. Huston *et al.*, Splenectomy inactivates the cholinergic antiinflammatory pathway during lethal endotoxemia and polymicrobial sepsis. *J. Exp. Med.* **203**, 1623–1628 (2006).
6. M. Rosas-Ballina *et al.*, Splenic nerve is required for cholinergic antiinflammatory pathway control of TNF in endotoxemia. *Proc. Natl. Acad. Sci. U.S.A.* **105**, 11008–11013 (2008).
7. G. Vida, G. Peña, E. A. Deitch, L. Ulloa, α7-cholinergic receptor mediates vagal induction of splenic norepinephrine. *J. Immunol.* **186**, 4340–4346 (2011).
8. A. M. Kressel *et al.*, Identification of a brainstem locus that inhibits tumor necrosis factor. *Proc. Natl. Acad. Sci. U.S.A.* **117**, 29803–29810 (2020).
9. Y. A. Levine *et al.*, Neurostimulation of the cholinergic anti-inflammatory pathway ameliorates disease in rat collagen-induced arthritis. *PLoS One* **9**, e104530 (2014).
10. J. Meregnani *et al.*, Anti-inflammatory effect of vagus nerve stimulation in a rat model of inflammatory bowel disease. *Auton. Neurosci.* **160**, 82–89 (2011).
11. S. J. Wilks *et al.*, Non-clinical and pre-clinical testing to demonstrate safety of the barostim neo electrode for activation of carotid baroreceptors in chronic human implants. *Front. Neurosci.* **11**, 438 (2017).
12. I. Gupta *et al.*, Quantification of clinically applicable stimulation parameters for precision near-organ neuromodulation of human splenic nerves. *Commun. Biol.* **3**, 577 (2020).
13. F. A. Koopman *et al.*, Vagus nerve stimulation inhibits cytokine production and attenuates disease severity in rheumatoid arthritis. *Proc. Natl. Acad. Sci. U.S.A.* **113**, 8284–8289 (2016).

14. M. C. Genovese *et al*., Safety and efficacy of neurostimulation with a miniaturised vagus nerve stimulation device in patients with multidrug-refractory rheumatoid arthritis: A two-stage multicentre, randomised pilot study. *Lancet Rheumatol.* **2**, e527–e538 (2020).
15. N. Stakenborg *et al*., Comparison between the cervical and abdominal vagus nerves in mice, pigs, and humans. *Neurogastroenterol. Motil.* **32**, e13889 (2020).
16. A. Handforth *et al*., Vagus nerve stimulation therapy for partial-onset seizures: A randomized active-control trial. *Neurology* **51**, 48–55 (1998).
17. B. Bonaz *et al*., Chronic vagus nerve stimulation in crohn's disease: A 6-month follow-up pilot study. *Neurogastroenterol. Motil.* **28**, 948–953 (2016).
18. E. Ben-Menachem, Vagus nerve stimulation, side effects, and long-term safety. *J. Clin. Neurophysiol.* **18**, 415–418 (2001).
19. D. Martelli, S. T. Yao, M. J. McKinley, R. M. McAllen, Reflex control of inflammation by sympathetic nerves, not the vagus. *J. Physiol.* **592**, 1677–1686 (2014).
20. Y. A. Patel, T. Saxena, R. V. Bellamkonda, R. J. Butera, Kilohertz frequency nerve block enhances anti-inflammatory effects of vagus nerve stimulation. *Sci. Rep.* **7**, 39810 (2017).
21. E. N. Nicolai *et al*., Sources of off-target effects of vagus nerve stimulation using the helical clinical lead in domestic pigs. *J. Neural Eng.* **17**, 046017 (2020).
22. D. Martelli, M. J. McKinley, R. M. McAllen, The cholinergic anti-inflammatory pathway: A critical review. *Auton. Neurosci.* **182**, 65–69 (2014).
23. V. Cotero *et al*., Noninvasive sub-organ ultrasound stimulation for targeted neuromodulation. *Nat. Commun.* **10**, 952 (2019).
24. M. Guyot *et al*., Apical splenic nerve electrical stimulation discloses an anti-inflammatory pathway relying on adrenergic and nicotinic receptors in myeloid cells. *Brain Behav. Immun.* **80**, 238–246 (2019).
25. N. R. Borley, J. M. McFarlane, H. Ellis, A comparative study of the tortuosity of the splenic artery. *Clin. Anat.* **8**, 219–221 (1995).
26. P. A. Sylvester, R. Stewart, H. Ellis, Tortuosity of the human splenic artery. *Clin. Anat.* **8**, 214–218 (1995).
27. C. G. J. Cleypool, D. Lotgeringk Bruinenberg, T. Roeling, E. Irwin, R. Bleys, Splenic artery loops: Potential splenic plexus stimulation sites for neuroimmunomodulatory based anti-inflammatory therapy? *Clin. Anat.* **34**, 371–380 (2020).
28. U. Heusermann, H. J. Stutte, Electron microscopic studies of the innervation of the human spleen. *Cell Tissue Res.* **184**, 225–236 (1977).
29. T. J. M. Verlinden *et al*., Innervation of the human spleen: A complete hilum-embedding approach. *Brain Behav. Immun.* **77**, 92–100 (2019).
30. D. B. Hoover, T. C. Brown, M. K. Miller, J. B. Schweitzer, D. L. Williams, Loss of sympathetic nerves in spleens from patients with end stage sepsis. *Front. Immunol.* **8**, 1712 (2017).
31. S. Huang *et al*., Lymph nodes are innervated by a unique population of sensory neurons with immunomodulatory potential. *Cell* **184**, 441–459.e25 (2021).
32. B. M. Assas, J. I. Pennock, J. A. Miyan, Calcitonin gene-related peptide is a key neurotransmitter in the neuro-immune axis. *Front. Neurosci.* **8**, 23 (2014).
33. T. Mózes *et al*., Protective effect of diclofenac sodium against endotoxic shock in anaesthetized pigs. *Prostaglandins Leukot. Essent. Fatty Acids* **48**, 193–200 (1993).
34. E. M. Schrauwen, A. M. Houvenaghel, Endotoxin shock in the pig: Beneficial effects of pretreatment with prednisolone sodium succinate. *Am. J. Vet. Res.* **45**, 1650–1653 (1984).
35. M. J. Myers, D. E. Farrell, D. C. Palmer, L. O. Post, Inflammatory mediator production in swine following endotoxin challenge with or without co-administration of dexamethasone. *Int. Immunopharmacol.* **3**, 571–579 (2003).
36. M. Kohoutova *et al*., Vagus nerve stimulation attenuates multiple organ dysfunction in resuscitated porcine progressive sepsis. *Crit. Care Med.* **47**, e461–e469 (2019).
37. J. Dalli, R. A. Colas, H. Arnardottir, C. N. Serhan, Vagal regulation of group 3 innate lymphoid cells and the immunoresolvent PCTR1 controls infection resolution. *Immunity* **46**, 92–105 (2017).
38. D. M. Sokal *et al*., Splenic nerve neuromodulation reduces inflammation and promotes resolution in chronically implanted pigs. *Front. Immunol.*, 10.3389/fimmu.2021.649786 (2021).
39. E. R. Kandel, J. H. Schwartz, T. Jesell, *Principles of Neural Science* (McGraw-Hill, New York, 2000).
40. H. C. Shin, Y. L. Lee, H. Y. Kwon, H. J. Park, S. A. Raymond, Activity-dependent variations in conduction velocity of C fibers of rat sciatic nerve. *Neurosci. Res.* **19**, 427–431 (1994).
41. C. V. Greenway, A. E. Lawson, R. D. Stark, Vascular responses of the spleen to nerve stimulation during normal and reduced blood flow. *J. Physiol.* **194**, 421–433 (1968).
42. B. N. Davies, J. Gamble, P. G. Withrington, Frequency-dependent differences in the responses of the capsular and vascular smooth muscle of the spleen of the dog to sympathetic nerve stimulation. *J. Physiol.* **228**, 13–25 (1973).
43. A. B. Ayers, B. N. Davies, P. G. Withrington, Responses of the isolated, perfused human spleen to sympathetic nerve stimulation, catecholamines and polypeptides. *Br. J. Pharmacol.* **44**, 17–30 (1972).
44. D. Granaat, The spleen in the regulation of the arterial blood pressure. *J. Physiol.* **122**, 209–218 (1953).
45. C. Risöe, W. Tan, O. A. Smiseth, Effect of carotid sinus baroreceptor reflex on hepatic and splenic vascular capacitance in vagotomized dogs. *Am. J. Physiol.* **266**, H1528–H1533 (1994).
46. D. Bakovic *et al*., Spleen volume and blood flow response to repeated breath-hold apneas. *J. Appl. Physiol.* **95**, 1460–1466 (2003).
47. D. M. Nance, J. Burns, Innervation of the spleen in the rat: Evidence for absence of afferent innervation. *Brain Behav. Immun.* **3**, 281–290 (1989).
48. N. L. Herman, D. R. Kostreva, J. P. Kampine, Splenic afferents and some of their reflex responses. *Am. J. Physiol.* **242**, 247–254 (1982).
49. A. Niijima, The afferent discharges from sensors for interleukin 1 beta in the hepatoportal system in the anesthetized rat. *J. Auton. Nerv. Syst.* **61**, 287–291 (1996).
50. P. B. Yoo *et al*., High-resolution measurement of electrically-evoked vagus nerve activity in the anesthetized dog. *J. Neural Eng.* **10**, 026003 (2013).